Geophys. J. Int. (2000) **140,** 147–157

Absorbing boundary and free-surface conditions in the phononic lattice solid by interpolation

Lian-Jie Huang,[1,*] Peter Mora[2,*] and Michael C. Fehler[1]

[1] *Los Alamos Seismic Research Center, EES Division, Mail Stop* D443, *Los Alamos National Laboratory, Los Alamos,* NM 87545, *USA. E-mail: ljh@lanl.gov*

[2] *Department of Earth Sciences, The University of Queensland, St. Lucia, Brisbane, Queensland* 4072, *Australia*

Accepted 1999 August 13. Received 1999 May 6; in original form 1996 August 22

SUMMARY

We have recently developed a new lattice-Boltzmann-based approach for modelling compressional wave propagation in heterogeneous media, which we call the phononic lattice solid by interpolation (PLSI). In this paper, we propose an absorbing boundary condition for the PLSI method in which the microscopic reflection coefficients at the boundaries of a model are set to zero and viscous layers are added to the boundaries. Numerical simulation examples using the PLSI method and comparisons with exact solutions demonstrate that artificial boundary reflections can be almost completely eliminated when the incidence angle is less than approximately 70°. Beyond this angle, remanent artificial boundary reflections become visible.

We propose four methods for modelling free-surface reflections in PLSI simulations. In the first three methods, special collision rules at a free surface are specified to take into account the effect of a free surface on quasi-particle movements (i.e. wave propagation). They are termed the specular bouncing, backward bouncing I, and combined bouncing methods. They involve quasi-particle reflections with a coefficient of -1 and require the free surface to be located exactly along lattice nodes. For the fourth method, we modify the backward bouncing I model for the case when a free surface is located at any position along lattice links and thus term it the backward bouncing II model. It uses the reflection coefficient at the free surface to calculate the reflected number densities during PLSI simulations. Hence, the free surface is handled in the same way as an interface within a model. Numerical examples and comparisons with exact solutions show that these four methods used at the microscopic scale are all appropriate for modelling macroscopic waves reflected from free surfaces.

Key words: absorbing boundary condition, compressional wave, free surface, lattice Boltzmann, phononic lattice solid, wave propagation.

1 INTRODUCTION

Classical numerical schemes for simulating wave propagation such as finite difference methods are based on discretizations of wave equations that are macroscopic continuum equations. The lattice Boltzmann method is a microscopic method in which the physical processes at the microscopic scale are simulated. It has recently been developed as an alternative numerical scheme for modelling fluid flows, particularly for those involving interfacial dynamics and complex boundaries (for an overview see Chen & Doolen 1998). Mora (1992) first introduced the lattice Boltzmann method into seismology to simulate wave propagation in heterogeneous media. In Mora's method, a finite difference scheme is used to solve the lattice solid Boltzmann equation and it is thus referred to as a semi-microscopic approach (Maillot 1994). Mora's method has the same limitations of finite difference schemes for simulating wave propagation. The phononic lattice solid by interpolation (PLSI) method is a lattice-Boltzmann-based approach for simulating compressional wave propagation in heterogeneous media (Huang 1994; Huang & Mora 1994a). Huang & Mora (1994a) showed that while no partial differential equations are directly solved in the PLSI method, the macroscopic limit of the method leads to the acoustic wave equation for

* Formerly at: Departement de Sismologie, Institut de Physique du Globe de Paris, 4 Place Jussieu, 75252 Paris Cedex 05, France.

heterogeneous media. The PLSI method has been used to simulate wave propagation in strongly heterogeneous media such as finely layered media, media with aligned heterogeneities and empty pores (Huang & Mora 1996). The method has also been extended to simulate non-linear solid–fluid interactions during wave propagation (Huang & Mora 1994b). In the PLSI method, the physical processes of wave propagation, including transportation, transmission, reflection and collision of quasi-particles carrying wavefields, are simulated at the microscopic scale. In PLSI simulations, (sharp) interfaces can be located at any position along lattice links. Like classical finite difference methods used to solve partial differential wave equations, PLSI simulations are performed in a model with finite dimensions due to computer memory size limitations. Therefore, absorbing boundary conditions must be imposed at the boundaries of the model to simulate wave propagation in an unbounded (i.e. 'infinite') medium.

Several kinds of absorbing boundary conditions have been developed for finite difference methods to solve partial differential wave equations (e.g. Clayton & Engquist 1977; Reynolds 1978; Keys 1985; Dablain 1986; Higdon 1991; Peng & Toksöz 1994). The best of these methods are successful (reflected wave amplitude is not larger than 5 per cent of incident wave amplitude) at eliminating boundary reflections for incidence angles up to about 40° (Higdon 1991) and 60° (Peng & Toksöz 1994). However, these methods are not directly applicable to PLSI simulations because no partial differential equations are directly solved in the PLSI method. Therefore, a new absorbing boundary condition must be designed for this method. We introduce an absorbing boundary condition that gives zero-valued microscopic reflection coefficients at the boundaries of a model and adds additional viscous layers at the boundaries in order to reduce artificial boundary reflections. Numerical examples are given to demonstrate the ability of the absorbing boundary condition to eliminate artificial boundary reflections.

Free surfaces such as the surface of the ocean or Earth are often required in wave propagation problems. Several kinds of free-surface conditions have been developed for classical finite difference or Chebychev spectral methods (e.g. Rodrigues & Mora 1993; Tessmer & Kosloff 1994). Like the case of absorbing boundary conditions, these are not directly applicable to the PLSI method because no partial differential equations are directly solved in the PLSI method. We propose four methods for modelling free-surface reflections. The first three methods are based on a modification of the quasi-particle collision process. They are analogous to the methods for modelling interactions of lattice gas particles with solid boundaries proposed by Lavallée *et al.* (1991) [other boundary conditions for the lattice gas and lattice Boltzmann methods can be found in Cornubert *et al.* (1991) and Ziegler (1993)]. These methods require a free surface to be exactly located along lattice nodes. A fourth approach requires a modification of the scattering step (that is, reflection step, because no transmission occurs at the free surface) to simulate reflections from a free surface that occurs between lattice nodes. This method allows a free surface to be located at any position on a lattice. Numerical examples using these methods demonstrate their ability to simulate free-surface reflections accurately. The results of PLSI simulations are compared with analytical solutions and we find a close agreement between the two. A detailed comparison among the PLSI method, analytical and other known solutions is given by Huang & Fehler (1998).

2 THE PHONONIC LATTICE SOLID BY INTERPOLATION

In this section, we give a brief description of the PLSI method (Huang 1994; Huang & Mora 1994a). The method is a lattice-Boltzmann-based approach to wave propagation in heterogeneous acoustic media. It is similar to the lattice gas method that is used to model idealized gas particles, but differs fundamentally in that quasi-particles in the PLSI method carry wavefields rather than mass and propagate through a heterogeneous medium. The PLSI simulates the physical processes of wave propagation. The number density of quasi-particles at each time step is obtained by calculating the contributions of four steps: (1) transportation step (movement along the links between lattice nodes), (2) transmission step, (3) reflection step, and (4) collision step.

2.1 Transportation step

We first consider the case when a lattice link is homogeneous so the transmission and reflection steps are not required. For the 2-D PLSI method, we use a triangular lattice with each node on the lattice connected to other nodes located at equally spaced 60° azimuths. For the transportation step of quasi-particles along a homogeneous lattice link in the α-direction ($\alpha = 1, 2, \ldots, 6$), there is a group of subnodes between each pair of nodes, as shown in Fig. 1(a). The spacing of the subnodes is chosen such that quasi-particles move from one

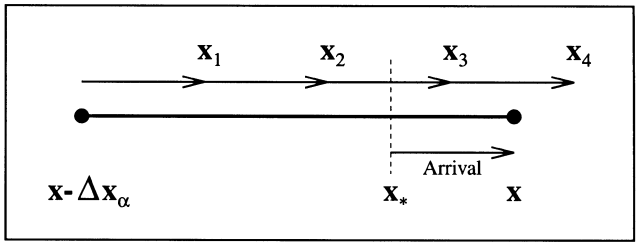

(a) Quasi-particle movement along a homogeneous link.

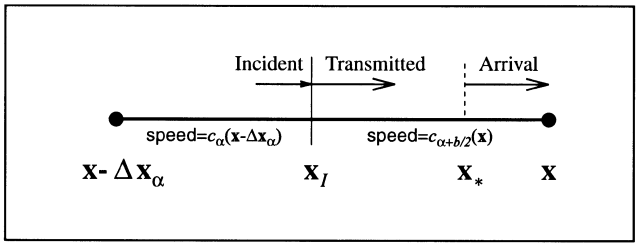

(b) Quasi-particle transmission along a heterogeneous link.

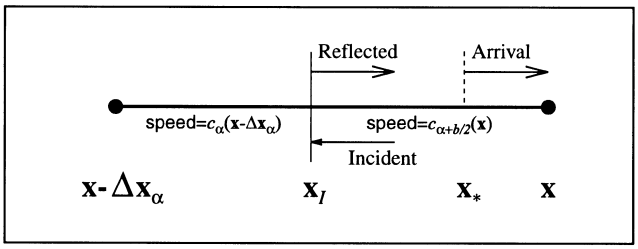

(c) Quasi-particle reflection along a heterogeneous link.

Figure 1. Illustration of quasi-particle movement along a lattice link. In (b) and (c), the interface is located at $\mathbf{x}_I$, which can be at any location between lattice nodes $\mathbf{x}-\Delta\mathbf{x}_\alpha$ and $\mathbf{x}$.

subnode to the next in each time step Δt. Thus, the subnode spacing varies spatially as velocity varies. In Fig. 1(a), the lattice nodes are located at $\mathbf{x}-\Delta\mathbf{x}_\alpha$ and $\mathbf{x}$, and the subnodes are located at $\mathbf{x}_1$, $\mathbf{x}_2$, ..., etc. Quasi-particles at $\mathbf{x}-\Delta\mathbf{x}_\alpha$ move to $\mathbf{x}_1$ in one time step. During subsequent time steps, quasi-particles move to $\mathbf{x}_2$, $\mathbf{x}_3$, etc. Therefore, at time t, the number density at $\mathbf{x}_j$ ($j=1, 2, \ldots$) is given by

$$\widetilde{N}_\alpha(\mathbf{x}_j, t)=N_\alpha(\mathbf{x}-\Delta\mathbf{x}_\alpha, t-j\Delta t)\,. \tag{1}$$

The quasi-particles at $\mathbf{x}_*$ will move to lattice node at $\mathbf{x}$ during the next time step and their number density $\widetilde{N}_\alpha(\mathbf{x}_*, t)$ is calculated by interpolating the number densities of quasi-particles at the surrounding subnodes. The contribution of the transportation step to the number density of quasi-particles moving in the α-direction at $\mathbf{x}$ at time $t+\Delta t$ is therefore given by

$$\widetilde{N}_\alpha(\mathbf{x}, t+\Delta t)=\widetilde{N}_\alpha(\mathbf{x}_*, t)\,. \tag{2}$$

For the movement of quasi-particles in the α-direction along a homogeneous lattice link between lattice nodes at $\mathbf{x}$ and $\mathbf{x}+\Delta\mathbf{x}_\alpha$, a new set of subnodes is set up along the lattice link and the number density at $\mathbf{x}+\Delta\mathbf{x}_\alpha$ is calculated in the same manner as described above for calculating the number density at $\mathbf{x}$ using the number density at $\mathbf{x}-\Delta\mathbf{x}_\alpha$. For each node on the triangular lattice, such calculations are conducted for each of the homogeneous lattice links along six directions.

2.2 Transmission and reflection steps

For the case when a lattice link is inhomogeneous, that is, there is an interface at some location along the lattice link, transmission and reflection steps must be taken into account during quasi-particle movements along the lattice link. These steps account for the changes caused by spatial variations in velocity and/or density (Figs 1b and c). As illustrated in Fig. 1(b), quasi-particles move from $\mathbf{x}-\Delta\mathbf{x}_\alpha$ in the α-direction to the interface at $\mathbf{x}_I$ with a speed of $c_\alpha(\mathbf{x}-\Delta\mathbf{x}_\alpha)$, transmit through the interface where the number density of quasi-particles is multiplied by the transmission coefficient and then move to the lattice node at $\mathbf{x}$ with a speed $c_{\alpha+b/2}(\mathbf{x})$, which is the speed in the direction opposite to the α-direction, namely the speed on the other side of the interface. The transmission coefficient is obtained from

$$T_\alpha(\mathbf{x}-\Delta\mathbf{x}_\alpha;\,\mathbf{x})=\frac{2\,Z_{\alpha+b/2}(\mathbf{x})}{Z_{\alpha+b/2}(\mathbf{x})+Z_\alpha(\mathbf{x}-\Delta\mathbf{x}_\alpha)}\,, \tag{3}$$

where $Z_\alpha(\mathbf{x})=\rho(\mathbf{x})c_\alpha(\mathbf{x})/\sqrt{D}$ is the impedance, $\rho(\mathbf{x})$ is the medium density, $c_\alpha(\mathbf{x})/\sqrt{D}$ is the macroscopic wave speed of the medium (Mora 1992) and D is the number of space dimensions. Fig. 1(c) shows that quasi-particles move from $\mathbf{x}$ in the $\alpha+b/2$-direction to the interface at $\mathbf{x}_I$ with a speed $c_{\alpha+b/2}(\mathbf{x})$, are reflected by the interface where the number density of quasi-particles is multiplied by the reflection coefficient and then move to the lattice node at $\mathbf{x}$ with the same speed. The reflection coefficient is given by

$$\begin{aligned}R_{\alpha+b/2}(\mathbf{x};\,\mathbf{x}-\Delta\mathbf{x}_\alpha)&=-R_\alpha(\mathbf{x}-\Delta\mathbf{x}_\alpha;\,\mathbf{x})\\&=-\frac{Z_{\alpha+b/2}(\mathbf{x})-Z_\alpha(\mathbf{x}-\Delta\mathbf{x}_\alpha)}{Z_{\alpha+b/2}(\mathbf{x})+Z_\alpha(\mathbf{x}-\Delta\mathbf{x}_\alpha)}\,.\end{aligned} \tag{4}$$

The movements of quasi-particles along links between a lattice node and the interface are the same as that along a homogeneous link (Fig. 1a). Therefore, the same interpolation algorithm used for a homogeneous link can be used to obtain the number densities of the incident quasi-particles and those of the quasi-particles at $\mathbf{x}_*$ (i.e. $\widetilde{N}^{\mathrm{T}}_\alpha(\mathbf{x}_*, t)$ for the transmission and $\widetilde{N}^{\mathrm{R}}_\alpha(\mathbf{x}_*, t)$ for the reflection) that will arrive at $\mathbf{x}$ during the next time step. Each transmission and reflection step requires two interpolations. Huang & Mora (1994a) proposed two alternative ways to obtained the number densities of quasi-particles at $\mathbf{x}_*$ using only one interpolation for each transmission and reflection step.

2.3 Collision step

Quasi-particles arriving at a lattice node from different directions at the same time collide with each other. After the collision processes, the number density $N_\alpha(\mathbf{x}, t+\Delta t)$ of quasi-particles moving in the α-direction at $\mathbf{x}$ at time $t+\Delta t$ is given by

$$N_\alpha(\mathbf{x}, t+\Delta t)=\widetilde{N}_\alpha(\mathbf{x}_*, t)+\Delta N^{\mathrm{c}}_\alpha(\mathbf{x}, t)\,, \tag{5}$$

where $\alpha=1, 2, \ldots, 6$. For an inhomogeneous lattice link, $\widetilde{N}_\alpha(\mathbf{x}_*, t)$ in eq. (5) is given by

$$\widetilde{N}_\alpha(\mathbf{x}_*, t)=\widetilde{N}^{\mathrm{T}}_\alpha(\mathbf{x}_*, t)+\widetilde{N}^{\mathrm{R}}_\alpha(\mathbf{x}_*, t)\,, \tag{6}$$

where the terms $\widetilde{N}^{\mathrm{T}}_\alpha$ and $\widetilde{N}^{\mathrm{R}}_\alpha$ are the transmitted and reflected number densities, respectively. In eq. (5), the term $\Delta N^{\mathrm{c}}_\alpha(\mathbf{x}, t)$ is the rate of change of the quasi-particle number density due to the collision process (see Higuera 1988),

$$\Delta N^{\mathrm{c}}_\alpha(\mathbf{x}, t)=\sum_{S,S'}(S'_\alpha-S_\alpha)A(S\to S')\prod_\beta n_\beta^{S_\beta}(1+n_\beta)^{S'_\beta}\,, \tag{7}$$

with

$$n_\beta=d+N_\beta(\mathbf{x}, t)\quad(\beta=1, 2, \ldots, b)\,, \tag{8}$$

where the term d is the background number density, the number density N_β of quasi-particles carrying wavefields is a small perturbation relative to the background number density d, and the Boolean variables S_α and S'_α define input and output states with a transition probability of $A(S\to S')$. The input configuration is characterized by a set of numbers $S=\{S_\alpha\}$, with $S_\alpha=0$ or 1 for $\alpha=1, 2, \ldots, 6$, that indicates whether the direction α contributes any particles to the collision ($S_\alpha=1$) or not ($S_\alpha=0$). Analogously, $S'=\{S'_\alpha\}$ with $S'_\alpha=0$ or 1 for $\alpha=1, 2, \ldots, 6$ indicates the distribution of the outgoing particles among all directions of the lattice.

We use the first set of Frisch–Hasslacher–Pomeau collision rules (referred to as the FHP-I collision rules) (see Frisch *et al.* 1986) for the 2-D case (see Fig. 2). These rules account for the head-on double collisions and the symmetric triple collisions. For instance, the collision term for the direction $\alpha=1$ is given by

$$\begin{aligned}\Delta N^{\mathrm{c}}_1(\mathbf{x}, t)=&\frac{1}{2}\left[-n_1n_4(h_2h_5+h_3h_6)+h_1h_4(n_2n_5+n_3n_6)\right]\\&+\frac{1}{3}\left(n_2n_4n_6h_1h_3h_5-h_2h_4h_6n_1n_3n_5\right)\,,\end{aligned} \tag{9}$$

with

$$h_\alpha=1+n_\alpha\quad(\alpha=1, 2, \ldots, 6)\,. \tag{10}$$

The terms in eq. (9) account for the collision process described in the following. The first term is the result of the head-on collision of quasi-particles arriving in the 1- and 4-directions

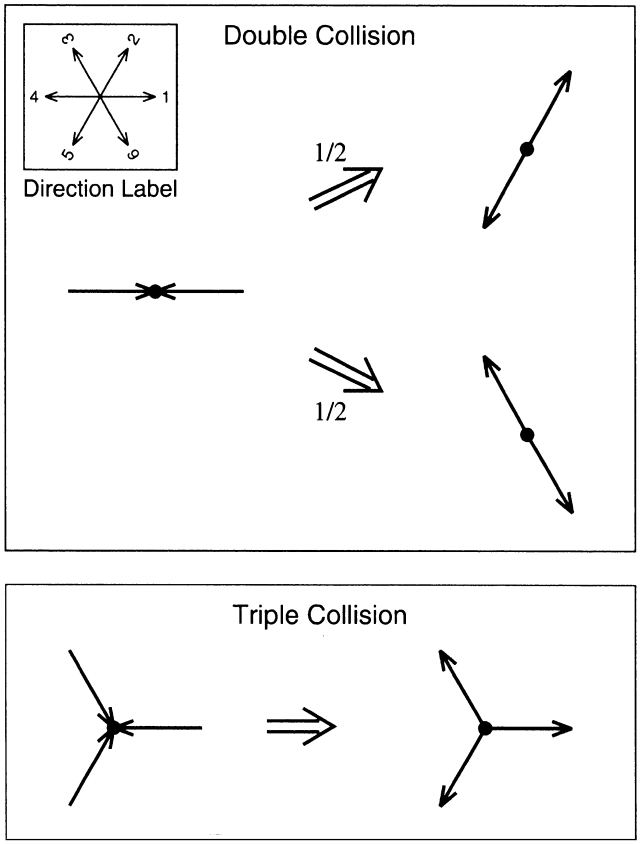

Figure 2. Illustration of the FHP-I collision rules: head-on double collision (upper panel) and symmetric triple collision (lower panel).

and leaving in both the 2- and 5-directions and the 3- and 6-directions with a transition probability of 1/2 after the collision (see Fig. 2). Since this collision process removes particles from the 1-direction, the term is negative. The second term is the increase in number density in the 1-direction due to the head-on collisions of particles arriving from the 2- and 5-directions and the 3- and 6-directions. The third and fourth terms account for symmetric triple collisions. The third term is the collision of particles arriving in the 2-, 4- and 6-directions that scatter into the 1-, 3- and 5-directions (see Fig. 2). This term is positive since it adds number density in the 1-direction. The last term is for particles arriving from the 1-, 3- and 5-directions that scatter into the 2-, 4- and 6-directions. This removes particles from the 1-direction. The transition probabilities for the FHP-I rules are 1/2 for head-on collisions and 1/3 for symmetric triple collisions. The rate of change of the number density in other directions due to the FHP-I collisions can be obtained by rotating the subscripts of physical quantities in eq. (9).

Higuera (1988) showed that the viscosity v of the medium is related to the value of d by

$$v = \frac{1}{12d(1+d)} - \frac{1}{8}. \tag{11}$$

Eq. (11) indicates that the viscosity vanishes for $d = \sqrt{11/12} - 1/2 \approx 0.457427$. We usually choose the value of d appropriate for zero viscosity. However, we will use a non-zero viscosity as part of our absorbing boundary condition.

In the macroscopic limit, the PLSI method leads to the acoustic wave equation for heterogeneous media (Huang & Mora 1994a). The advantage of the PLSI method is that it can easily handle models with sharp interfaces, complex surface topography and strong velocity contrast inclusions, including cavities. These features are very difficult for classical finite difference solutions to the wave equation to simulate reliably. An extension of the PLSI method, termed the phononic lattice solid with fluids, has been proposed and shown to be a reliable method for modelling seismic wave propagation in porous media where the pores contain fluids (Huang & Mora 1994b).

No PLSI version for elastic waves in heterogeneous media is available yet. Maillot (1994) developed a semi-microscopic approach for modelling elastic wave propagation in heterogeneous media. A finite difference scheme is used in Maillot's method. Recently, Qian & Deng (1997) used a lattice Bhatnager–Gross–Krook (BGK) model to simulate shear waves in a homogeneous viscous medium. Ultimately, it is necessary to develop a lattice-Boltzmann-based method capable of handling P waves, S waves and converted waves in heterogeneous media to simulate elastic wave propagation in solids at the microscopic scale.

3 ABSORBING BOUNDARY CONDITION

For a lattice node at a model boundary, no quasi-particles exist outside the model; therefore, there are no transmission and transportation steps at boundaries. Boundary artefacts arise only from the reflection and collision steps. To eliminate the contribution from the reflection step to these artefacts, we set the microscopic reflection coefficients to zero at boundaries. In the following, we perform a numerical test to study the effectiveness of zero-valued microscopic reflection coefficients.

3.1 Test of zero-valued reflection coefficients at absorbing boundaries

A homogeneous model defined on a 160×160 triangular lattice was used for the PLSI simulation. The quasi-particle speed was 0.4 and the density of the medium was 1.0. A pressure source with a first derivative of Gaussian time history was introduced at lattice node (80, 80). It had an amplitude of 0.010 and a time delay of 60 time steps. The fundamental frequency of the source was such that it generated waves with a wavelength of approximately 16 lattice spacings. Receivers were located along a horizontal line at a depth of 40 vertical lattice spacings from the upper boundary of the model. The background number density of quasi-particles is 0.457427. Zero-valued reflection coefficients were set at all boundaries of the model. Computations were made using the PLSI method for 900 time steps. Fig. 3(a) depicts the seismograms (i.e. pressure fields) recorded at the receivers, amplified by a factor of $t^{0.7}$, where t is the time step. In addition to the direct wave, one can see from Fig. 3(a) that some weak boundary reflections are still visible after the direct wave. This indicates that setting zero-valued reflection coefficients at boundaries is not adequate for eliminating the artificial boundary reflections. We will introduce viscous absorbing boundary layers to the model to further reduce these artefacts.

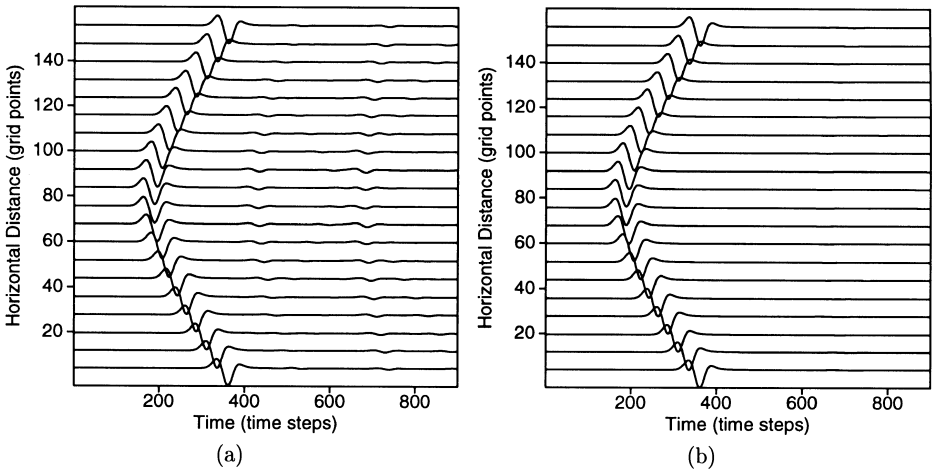

Figure 3. The amplified seismograms recorded during the PLSI calculations for a homogeneous model with (a) zero-valued microscopic reflection coefficients at the boundaries and (b) zero-valued microscopic reflection coefficients plus viscous boundary layers.

3.2 Viscous absorbing boundary layers

The only source of the artificial boundary reflections in Fig. 3(a) is the contribution of the quasi-particle collision process at the boundaries. We introduce a viscous layer at the absorbing boundaries in an attempt to reduce the amplitude of the artificial boundary reflections. The viscosity of a lattice solid model may be adjusted by selection of the background number density of quasi-particles. For a specified set of collision rules, a particular value of the background number density can be chosen such that the viscosity approaches zero (see eq. 11). When the background number density is less than this particular value, the viscosity becomes positive and its value increases as the background number density decreases. Beyond this value, the viscosity becomes negative (non-physical) and its absolute value increases with the background number density. Therefore, we add a viscous layer (i.e. a layer with positive viscosity) to the boundaries of a model to absorb the artificial boundary reflections by an appropriate choice of background number density. This layer is called a viscous absorbing boundary layer. To avoid the reflection from the 'interface' between the edge of a model and the edge of a viscous absorbing boundary layer (this interface is henceforth called a boundary interface), the viscosity of the absorbing boundary layer increases smoothly from zero (or the value of the medium) at the boundary interface up to a given value at the outer edge of the absorbing boundary layer. Numerically, the background number density of the boundary layer is varied using some smooth function such as a Hanning taper. In the calculations presented in this paper, we use a Hanning taper to vary the number density smoothly from 0.457427 in the interior region to zero at the boundary of the computational domain. The microscopic reflection coefficients at the outer edge of the boundary layer are set to zero.

A viscous boundary layer with a thickness of 40 vertical or horizontal lattice spacings was added to each boundary of the model used in the above numerical test and consequently the PLSI calculations were carried out on a 240×240 triangular lattice. The same pressure source used above was introduced at lattice node (120, 120). Receivers were located along a horizontal line at a depth of 80 vertical lattice spacings from the upper boundary of the model. No receivers were placed in absorbing boundary layers. All other parameters used in the PLSI simulation remained the same as those used in the first numerical test. Computations were made using the PLSI method for 900 time steps. The corresponding seismograms (i.e. pressure) recorded at the receivers are displayed in Fig. 3(b) at the same scale as Fig. 3(a). Artificial boundary reflections are no longer visible.

In summary, the absorbing boundary condition for the PLSI method is designed by

(1) setting the microscopic reflection coefficients at boundaries of a model to zero, and
(2) adding viscous layers to the boundaries.

Fig. 4 shows a comparison between the above seismograms obtained with the absorbing boundary condition and those obtained using an analytical solution of the 2-D acoustic wave equation for a homogeneous medium. No time amplification was used in the figure. It demonstrates that the PLSI solution agrees very well with the analytical solution.

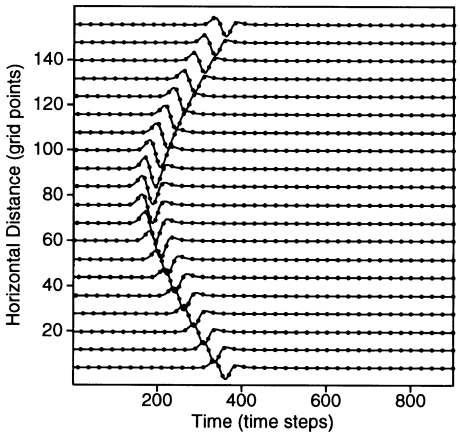

Figure 4. Comparison between the seismograms shown in Fig. 3(b) but without time amplification and those obtained using an analytical solution. Solid lines are for the PLSI solutions and dots are for the analytical solution.

4 INCIDENCE ANGLE DEPENDENCE OF THE ABSORBING BOUNDARY CONDITION

In the following, we study the incidence angle dependence of reflections from the absorbing boundary condition introduced above. The incidence angle β is defined as the angle between the boundary normal direction and the ray path, as shown in Fig. 5. A homogeneous model defined on an 80×320 triangular lattice without viscous absorbing boundary layers was used for the PLSI simulation of wave propagation. A pressure source with the same characteristics as the source used in the previous simulation was introduced at lattice node (40, 280). All other parameters were the same as those of the previous numerical examples. Receivers were located along horizontal lines at lattice depths of 280, 250, 200, 150 and 10 from the upper boundary of the model. The corresponding incidence angles β for boundary reflections recorded at receivers located at the right (or left) boundary of the model were 0.0°, 33.0°, 60.0°, 70.4° and 80.3°, respectively. Computations were made using the PLSI method for 1200 time steps. The seismograms are displayed in Figs 6(a1)–(e1) using a time-step-dependent gain of $t^{0.7}$.

Next, viscous boundary layers with the same thickness and properties as used in the PLSI simulation corresponding to Fig. 3(b) were added to all model boundaries. The PLSI computations with the absorbing boundary condition were made again for 1200 time steps. The corresponding amplified seismograms are displayed in Figs 6(a2)–(e2) at the same scale as used in Figs 6(a1)–(e1). Comparing each pair of figures, one can see that there are no visible boundary reflections in Figs 6(a2)–(c2) that correspond to the incidence angles of 0.0°–60°. For the case of the maximum incidence angle of 70.4° (Fig. 6d2), weak boundary reflections are visible but much smaller in amplitude than those in Fig. 6(d1). When the incidence angle increases up to 80.3° (Fig. 6e2), the boundary reflections from the left and right boundaries of the model become visible.

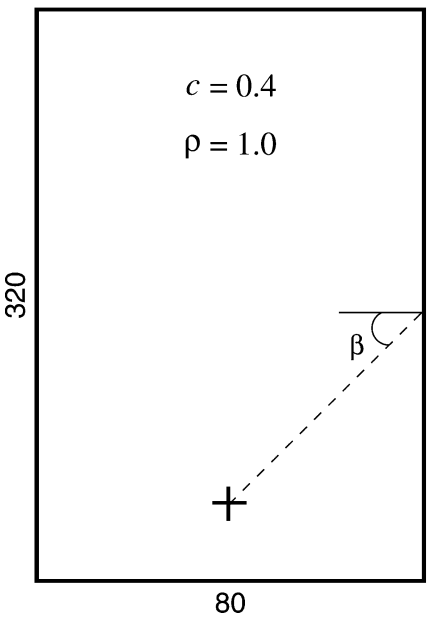

Figure 5. Schematic illustration of a homogeneous model without viscous absorbing boundary layers used for the study of the incidence angle dependence of the absorbing boundary condition. The plus sign represents the position of the pressure source and the angle β is the incidence angle at the right-hand boundary of the model.

5 FOUR METHODS FOR MODELLING FREE-SURFACE REFLECTIONS

It is important to model free-surface reflections when simulating wave propagation through realistic models of the Earth. Classical finite difference methods to solve partial differential wave equations describing wave phenomena in continuum media often have difficulty in handling free-surface boundary conditions, particularly when the free surface is irregular (Komatitsch *et al.* 1996; Ohminato & Chouet 1997). We propose four methods for modelling free-surface reflections in PLSI simulations (see Fig. 7). In each panel of Fig. 7, only a small part of a free surface in a 2-D triangular lattice is depicted. In the first method, quasi-particles arriving at a free surface in a certain direction will be specularly bounced back to another direction. We refer to this as the *specular bouncing* method. For example, as shown in Fig. 7(a), quasi-particles moving in direction 2 will be bounced to direction 6 (see lattice node A) and those moving in direction 3 will be bounced to direction 5 (see lattice node B). These reflections are performed with a change of sign in the number density perturbation.

An alternative method is termed *backward bouncing I* (see Fig. 7b). In this case, quasi-particles will be bounced back along the opposite direction to the incidence direction, coupled with a change in sign of the number density perturbation. For instance, quasi-particles moving in direction 2 will be bounced to direction 5 and those moving in direction 3 will be bounced to direction 6, as shown at lattice nodes A and B, respectively, in Fig. 7(b).

For the simulation of free-surface reflections, it seems that the specular bouncing method should be more suitable than the backward bouncing I method.

In lattice gas simulations, the corresponding so-called 'bounce-back' reflection method is commonly used for the study of interactions of fluid flows with solid boundaries (Lavallée *et al.* 1991). However, Lavallée *et al.* (1991) pointed out that there are good reasons to examine other types of reflections from solid boundaries. One reason stems from consideration of experiments at the molecular level. Knudsen (1934) conducted an experiment where molecules were directed towards a wall at a fixed incidence angle and observed that molecules were randomly scattered into all directions. In a lattice gas, this would correspond to a combination of the specular and bounce-back reflection methods. The second reason given by Lavallée *et al.* (1991) is that with purely deterministic interactions with the wall, the Boltzmann assumption that no correlation exists between particles prior to collision is not valid. Note, however, that the hypothesis is correct in a statistical sense for a combination of 50 per cent probability of the bounce-back method and 50 per cent probability of the specular reflection method.

When modelling free-surface reflections using the PLSI method, one way to account for the molecular observations of Knudsen (1934) is to combine the specular bouncing method and the backward bouncing I method to yield a third method (see Fig. 7c), which we term the *combined bouncing* method. In this case, quasi-particles arriving at the free surface in

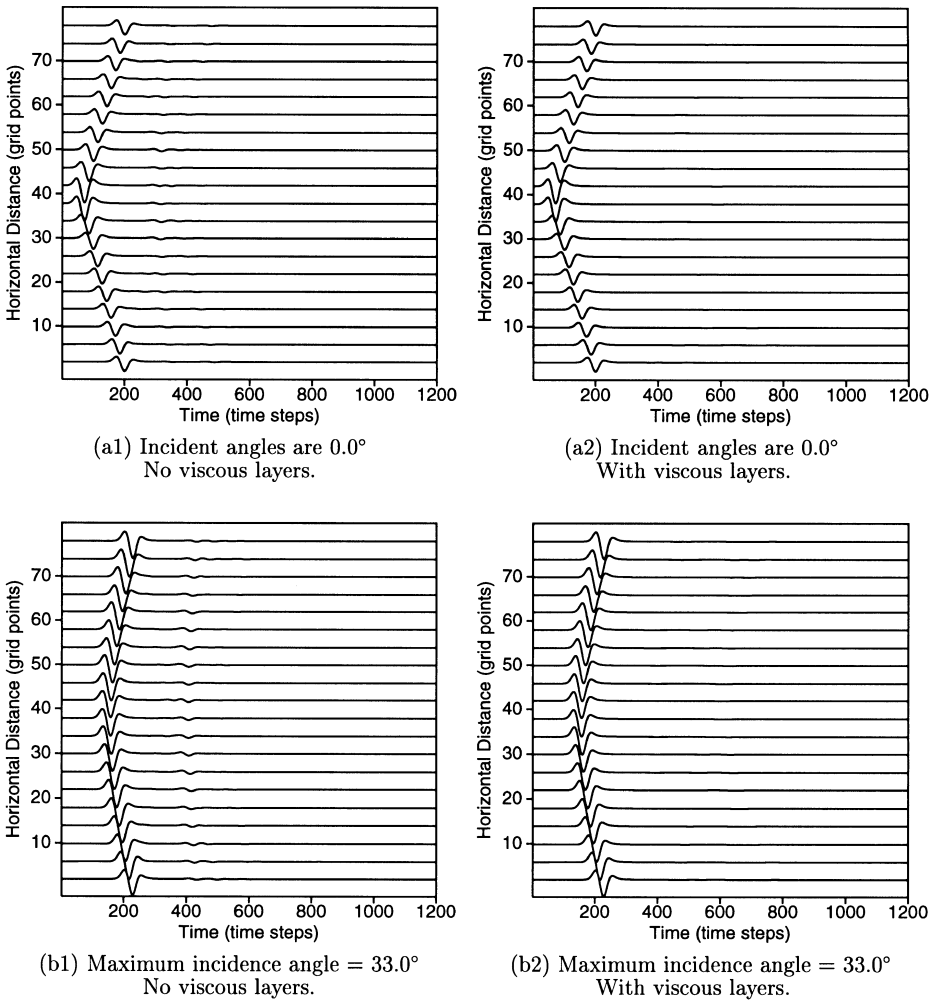

Figure 6. Comparisons of the amplified seismograms (i.e. pressure) recorded during the PLSI calculations to simulate wave propagation from a pressure source in a homogeneous model. (a1)–(e1) are results obtained using zero-valued microscopic reflection coefficients for a model defined on an 80×320 triangular lattice with a pressure source at lattice node (40, 280). (a2)–(e2) are the corresponding results obtained using viscous boundary layers in addition to zero-valued microscopic reflection coefficients. The maximum incidence angles are for boundary reflections recorded at receivers located at the left or right boundaries of the model.

directions 2 or 3 will be equally bounced back to directions 5 and 6 with a number density perturbation sign change, as shown, respectively, at lattice nodes A and B in Fig. 7(c). The above three methods can be considered as special collision rules for quasi-particles at a free surface.

When a free surface is not exactly located along lattice nodes, it is handled in the same way as interfaces within a model (see Fig. 7d). For example, as shown in Fig. 7(d), quasi-particles moving in direction 2 at lattice node A move to the free surface and are reflected back along direction 5 with a reflection coefficient of -1. Similarly, quasi-particles moving in direction 3 to the free surface are reflected backwards with a reflection coefficient of -1, as shown at lattice node B in Fig. 7(d). For this case, the process describing the quasi-particle behaviour at the free surface is similar to the backward bouncing I method. Therefore, this method for modelling free-surface reflections is termed the *backward bouncing II* method.

Note that in each of the above methods for modelling free-surface reflections, the process of quasi-particle interaction with a free surface can occur at lattice nodes at any location. Therefore, these methods do not have any particular restrictions on the shape of a free surface. In other words, these methods can be applied to plane or irregular free surfaces.

6 NUMERICAL SIMULATIONS OF FREE-SURFACE REFLECTIONS

A homogeneous medium defined on a 240×200 triangular lattice with a free surface at the upper boundary of the model and the absorbing boundary condition at the left, right and lower boundaries was used in all the following numerical examples to simulate free-surface reflections. Each viscous absorbing boundary layer has a thickness of 40 vertical or horizontal lattice spacings and the same properties as those used to calculate Figs 6(a2)–(e2). A pressure source with a first-derivative Gaussian time history, an amplitude of 0.010 and a time delay of 60 time steps was introduced at lattice node (120, 80). It generated waves with a wavelength of approximately 16 lattice spacings. The quasi-particle speed is 0.4 and

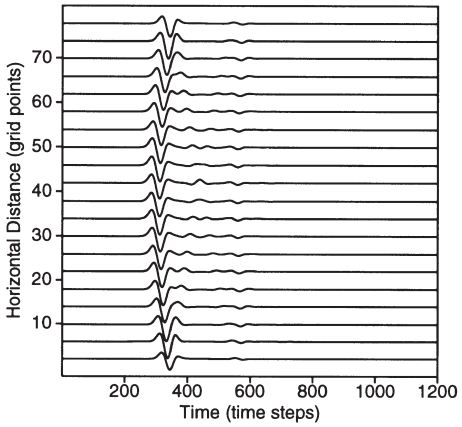

(c1) Maximum incidence angle = 60.0°
No viscous layers.

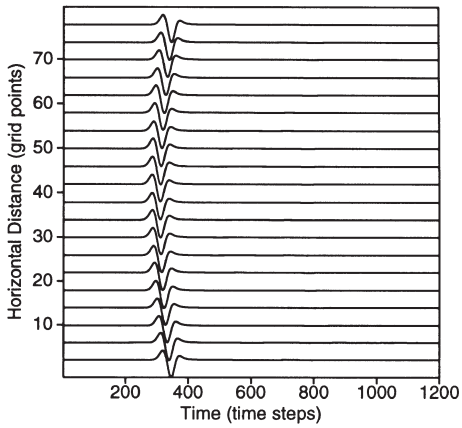

(c2) Maximum incidence angle = 60.0°
With viscous layers.

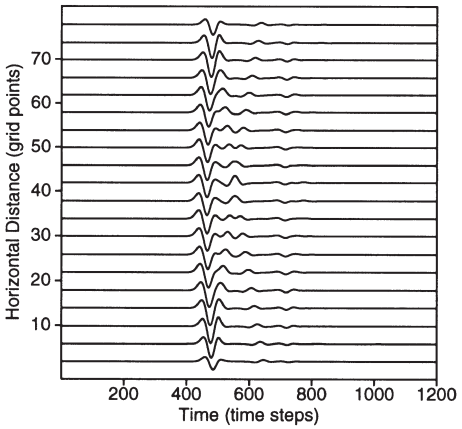

(d1) Maximum incidence angle = 70.4°
No viscous layers.

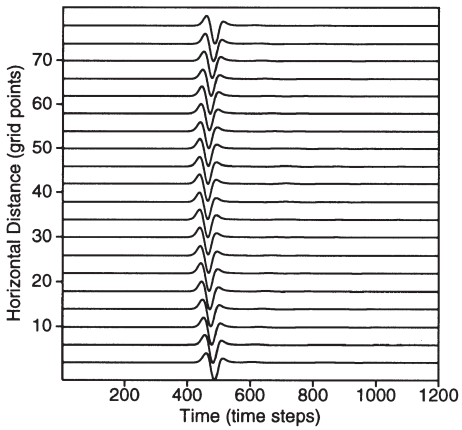

(d2) Maximum incidence angle = 70.4°
With viscous layers.

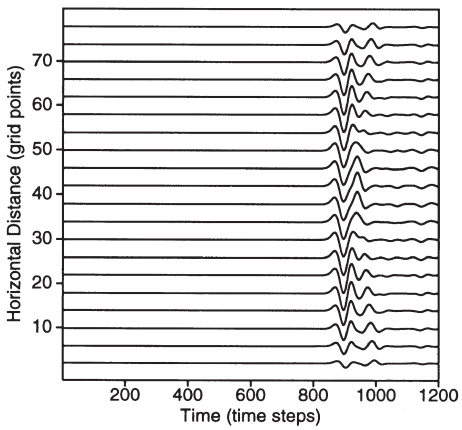

(e1) Maximum incidence angle = 80.3°
No viscous layers.

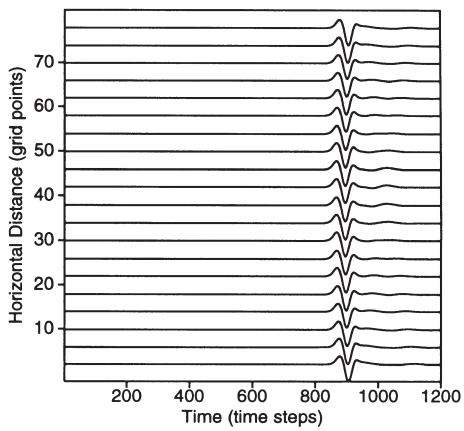

(e2) Maximum incidence angle = 80.3°
With viscous layers.

Figure 6. (*Continued.*)

the density of the medium is 1.0. The background number density of quasi-particles is 0.457427 so the viscosity approaches zero (see eq. 11). Seismograms were recorded at receivers located along a horizontal line at a depth of 40 vertical lattice spacings from the upper boundary of the model. No receivers were located in absorbing boundary layers. PLSI computations were run for 800 time steps.

First, the specular bouncing method was used during the PLSI simulation. The direct and reflected waves from the free surface can be identified in a snapshot of pressure at 350 time steps shown in Fig. 8, where the plus sign represents the position of the pressure source. The figure shows that the wave reflected from the free surface has changed its polarity relative to the incidence wave. The solid lines in Fig. 9(a) depict

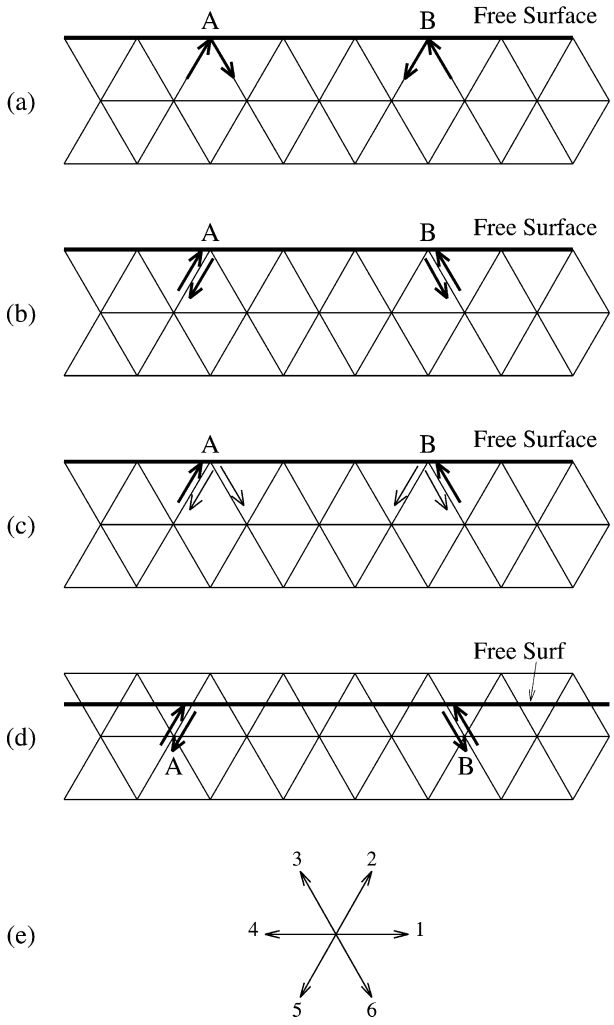

Figure 7. Illustration of four methods for modelling free-surface reflections in PLSI simulations. The specular bouncing (a), backward bouncing (b) and combined bouncing (c) methods are used when a free surface is located exactly along lattice nodes. The backward bouncing II (d) method is used when the free surface is located at any position on a lattice. All the bouncing processes are performed with a change in sign of the number density perturbation. (e) depicts the labelling of the lattice directions for a node on a 2-D grid.

the seismograms recorded at the receivers during the above PLSI simulation with the absorbing boundary condition. The lines show the direct waves and the reverse polarity waves reflected from the free surface as expected. In the next two PLSI simulations, the backward bouncing I and the combined bouncing methods were used respectively to simulate free-surface reflections. The corresponding seismograms showing pressure at the receivers are displayed in Figs 9(b) and (c) with solid lines.

For the case where the free surface was located along a horizontal line below the first row of the lattice with a distance of 1/2 vertical lattice spacing in the above model, the backward bouncing II method was used to simulate free-surface reflections. The resulting seismograms are displayed in Fig. 9(d) with solid lines.

Analytical solutions for all the above simulations are shown in Fig. 9 with dots. Comparisons between the PLSI solutions and the analytical solutions indicate that our four proposed methods can accurately model free-surface reflections during PLSI simulations.

7 CONCLUSIONS AND DISCUSSION

We have proposed an absorbing boundary condition for the PLSI method to simulate wave propagation in unbounded heterogeneous media. The microscopic reflection coefficients at boundaries of a model are set to zero. Viscous boundary layers are added to the model boundaries to absorb the remnants of artificial boundary reflections. Numerical examples demonstrate that artificial boundary reflections can be eliminated almost completely when the incidence angle is less than approximately 70°. Beyond this angle, the remanent artificial boundary reflections become visible.

We have four proposed methods for modelling free-surface reflections during PLSI simulations. The first three methods are termed the specular bouncing, the backward bouncing I and the combined bouncing methods. They are performed during the collision step of quasi-particles at a free surface. They can be used only when a free surface is located exactly along lattice nodes. Numerical examples demonstrate that, like methods to simulate interactions of fluid flows with solid boundaries in lattice gas simulations, not only is the specular bouncing method appropriate for modelling macroscopic free-surface reflections in PLSI simulations, but the backward bouncing and the combined bouncing methods are also applicable. In other words, at the microscopic scale it does not matter which one of the above methods is used for modelling free-surface reflections. Combinations of these methods can be used for modelling free-surface reflections when a free surface is located along lattice nodes but not lattice links. For cases where the free surface is located at any position on a lattice, we have proposed the backward bouncing II method to simulate free-surface reflections. It is carried out in the scattering step. Our four proposed methods for modelling free-surface reflections can be applied to both plane and irregular free surfaces.

The phononic lattice solid with fluids (PLSF) method (Huang 1994; Huang & Mora 1994b) is a lattice-Boltzmann-based method for modelling non-linear solid–fluid interactions. It takes into account lattice node movements induced by the passage of a macroscopic wave. Our proposed absorbing and free-surface conditions for the PLSI method are also suitable to the PLSF because both methods simulate the same microscopic physical processes of wave propagation, that is, transportation, reflection, transmission and collision of quasi-particles.

ACKNOWLEDGMENTS

We appreciate the valuable comments of Robert Geller and Heiner Igel. We thank Peter Roberts for his comments and careful reading of this manuscript. This research was funded partially by the sponsors of the Seismic Simulation Project at the Institut de Physique du Globe de Paris, and partially by the Laboratory Directed Research and Development program at the Los Alamos National Laboratory (LANL) under the auspices of the US Department of Energy through contract number W-7405-ENG-36. Calculations were performed at the Los Alamos National Laboratory Advanced Computing Laboratory. This paper is Los Alamos Seismic Research Center of LANL contribution No. 3.

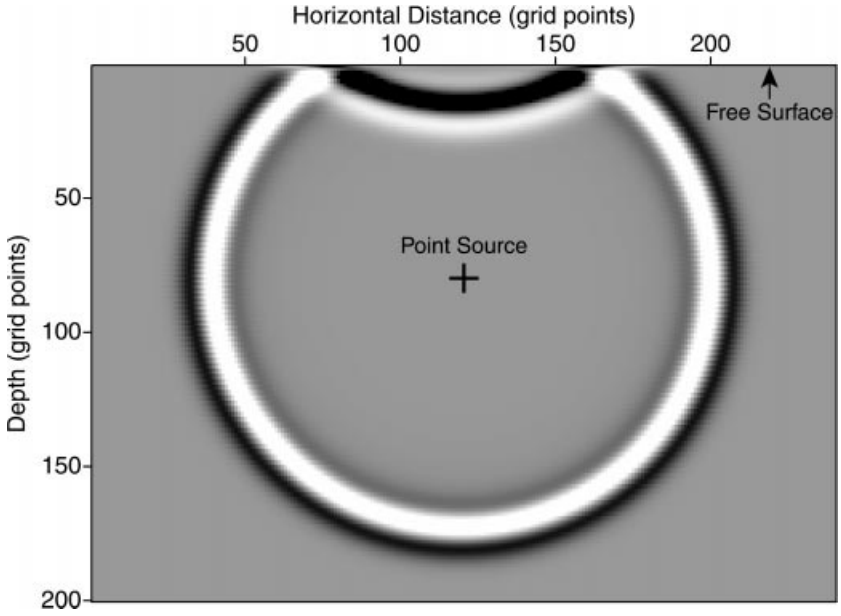

Figure 8. A snapshot at 350 time steps during the PLSI simulation to model free-surface reflections. The plus sign represents the position of the pressure source. The homogeneous model was defined on a 240×200 triangular lattice. No absorbing boundaries were used in this calculation. The specular bouncing method was used for modelling the free-surface reflections.

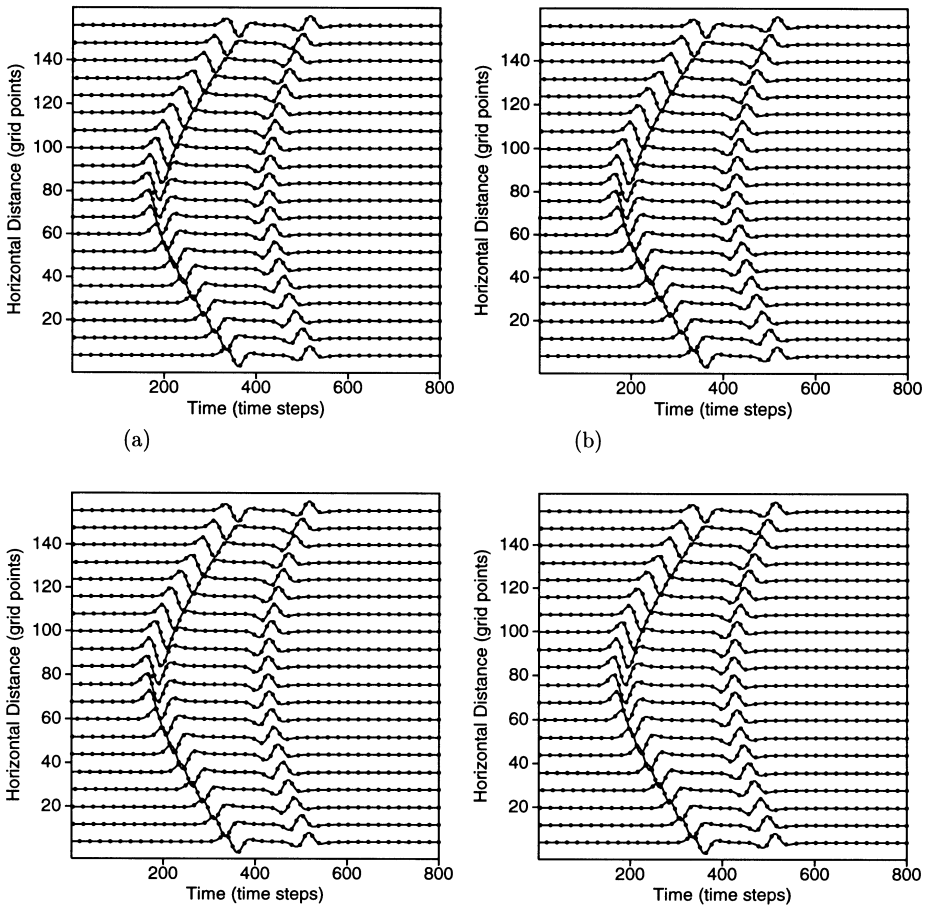

Figure 9. Seismograms (solid lines) recorded at receivers located at a depth of 40 vertical lattice spacings from the free surface during the PLSI simulations. The dots represent the corresponding analytical solutions. For the free-surface reflections during the PLSI simulations, the specular bouncing (a), backward bouncing I (b), combined bouncing (c) and backward bouncing II (d) methods were used.

REFERENCES

Chen, S. & Doolen, G.D., 1998. Lattice Boltzmann method for fluid flows, *Ann. Rev. Fluid Mech.,* **30,** 329–364.

Clayton, R. & Engquist, B., 1977. Absorbing boundary-conditions for acoustic and elastic wave-equations, *Bull. seism. Soc. Am.,* **67,** 1529–1540.

Cornubert, R., d'Humières, D. & Levermore, D., 1991. A Knudsen layer theory for lattice gases, *Physica D,* **47,** 241–259.

Dablain, M.A., 1986. The application of high-order differencing to the scalar wave equation, *Geophysics,* **51,** 54–66.

Frisch, U., Hasslacher, B. & Pomeau, Y., 1986. Lattice-gas automata for the Navier-Stokes equation, *Phys. Rev. Lett.,* **56,** 1505–1508.

Higdon, R.L., 1991. Absorbing boundary conditions for elastic waves, *Geophysics,* **56,** 231–241.

Higuera, F.J., 1988. Lattice gas simulation based on the Boltzmann equation, in *Discrete Kinetic Theory, Lattice Gas Dynamics and Foundations of Hydrodynamics,* pp. 162–177, ed. Monaco, R., World Scientific, Singapore.

Huang, L.-J., 1994. Microscopic approaches to wave propagation in complex media, *PhD thesis,* University of Paris 7.

Huang, L.-J. & Fehler, M.C., 1998. Accurate numerical modeling of wave propagation in strongly heterogeneous media using a lattice Boltzmann approach, *EOS, Trans. Am. geophys. Un,* **79**(5), F626.

Huang, L.-J. & Mora, P., 1994a. The phononic lattice solid by interpolation for modelling *P* waves in heterogeneous media, *Geophys. J. Int.,* **119,** 766–778.

Huang, L.-J. & Mora, P., 1994b. The phononic lattice solid with fluids for modelling non-linear solid–fluid interactions, *Geophys. J. Int.,* **117,** 529–538.

Huang, L.-J. & Mora, P., 1996. Numerical simulation of wave propagation in strongly heterogeneous media using a lattice solid approach, in *Mathematical Methods in Geophysical Imaging IV,* ed. Hassanzadeh, S., *Proc. SPIE,* **2282,** 170–179.

Keys, R.G., 1985. Absorbing boundary conditions for acoustic media, *Geophysics,* **50,** 892–902.

Knudsen, M., 1934. *The Kinetic Theory of Gases,* Methuen Monographs, London.

Komatitsch, D., Coutel, F. & Mora, P., 1996. Tensorial formulation of the wave-equation for modelling curved interfaces, *Geophys. J. Int.,* **127,** 156–168.

Lavallée, P., Boon, J.P. & Noullez, A., 1991. Boundaries in lattice gas flows, *Physica D,* **47,** 233–240.

Maillot, B., 1994. Semi-microscopic models of elastic waves, *PhD thesis,* University of Paris 7.

Mora, P., 1992. The lattice Boltzmann phononic lattice solid, *J. Stat. Phys.,* **68,** 591–609.

Ohminato, T. & Chouet, B., 1997. A free-surface boundary-condition for including 3D topography in the finite-difference method, *Bull. seism. Soc. Am.,* **87,** 494–515.

Peng, C. & Toksöz, M.N., 1994. An optimal absorbing boundary condition for finite difference modeling of acoustic and elastic wave propagation, *J. acoust. Soc. Am.,* **95,** 733–745.

Qian, Y.-H. & Deng, Y.-F., 1997. A lattice BGK model for viscoelastic media, *Phys. Rev. Lett.,* **79,** 2742–2745.

Reynolds, A.C., 1978. Boundary conditions for the numerical solution of wave propagation problems, *Geophysics,* **43,** 1099–1110.

Rodrigues, D. & Mora, P., 1993. An efficient implementation of the free surface boundary condition in the 2-D and 3-D elastic case, in *Expanded Abstracts, 63rd Annual Int. Mtg., Washington, DC,* pp. 215–217, SEG, Tulsa.

Tessmer, E. & Kossloff, D., 1994. 3-D elastic modeling with surface topography by a Chebychev spectral method, *Geophysics,* **59,** 464–473.

Ziegler, D.P., 1993. Boundary conditions for lattice Boltzmann simulations, *J. Stat. Phys.,* **71,** 1171–1177.